

## Accepted Manuscript

Spectral investigation and structural characterization of Dibenzalacetone :  $\beta$ -Cyclodextrin inclusion complex

R. Periasamy, R. Rajamohan, S. Kothainayaki, K. Sivakumar

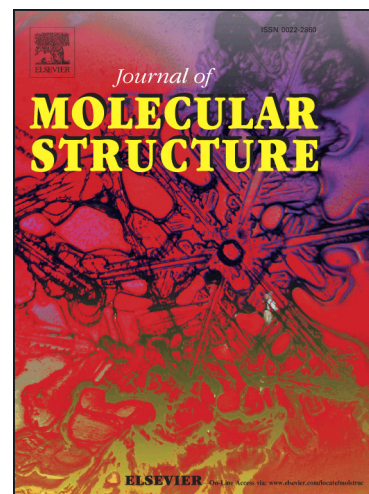
PII: S0022-2860(14)00357-3  
DOI: <http://dx.doi.org/10.1016/j.molstruc.2014.04.004>  
Reference: MOLSTR 20511

To appear in: *Journal of Molecular Structure*

Received Date: 25 October 2013  
Revised Date: 30 March 2014  
Accepted Date: 3 April 2014

Please cite this article as: R. Periasamy, R. Rajamohan, S. Kothainayaki, K. Sivakumar, Spectral investigation and structural characterization of Dibenzalacetone :  $\beta$ -Cyclodextrin inclusion complex, *Journal of Molecular Structure* (2014), doi: <http://dx.doi.org/10.1016/j.molstruc.2014.04.004>

This is a PDF file of an unedited manuscript that has been accepted for publication. As a service to our customers we are providing this early version of the manuscript. The manuscript will undergo copyediting, typesetting, and review of the resulting proof before it is published in its final form. Please note that during the production process errors may be discovered which could affect the content, and all legal disclaimers that apply to the journal pertain.



## Spectral investigation and structural characterization of Dibenzalacetone : $\beta$ -Cyclodextrin inclusion complex.

R. Periasamy<sup>1</sup>, R. Rajamohan<sup>2</sup>, S. Kothainayaki<sup>1\*</sup> and K. Sivakumar<sup>3</sup>

<sup>1</sup>Chemistry Section, FEAT, Annamalai University, Annamalai Nagar, Tamil Nadu, India – 608002

<sup>2</sup> Department of Chemistry, S.K.P. Institute of Technology, Tiruvannamalai- 606 611

<sup>3</sup> Department of Chemistry, Faculty of Science, SCSVMV University, Enathur, Kanchipuram 631 561, Tamilnadu

### Abstract

The interaction of Dibenzalacetone (DBA) with  $\beta$ -Cyclodextrin ( $\beta$ -CD) producing an inclusion complex was carried out by co-precipitation method. The binding constant was determined using steady state and time-resolved fluorescence spectroscopy and the results suggested that the inclusion complex preferred 1:1 stoichiometry. The complex is characterized by UV-Visible, infrared spectroscopy (FT-IR), differential scanning calorimetry (DSC) and X-ray diffractometry (XRD). The morphological characteristics of the solid complex were analyzed by Scanning electron microscope (SEM) and Atomic force microscope (AFM). The structure of 1:1 inclusion complex of DBA with  $\beta$ -CD is proposed. The Docking study reveals that this structure was found to be highly probable and potentially favorable model.

---

\*Corresponding author

Tel:- +91 9486456733

Email: [kothaichemish@yahoo.co.in](mailto:kothaichemish@yahoo.co.in) (S. Kothainayaki)

Keyword: . 1,5-Diphenyl-1,4-pentadien-3-one,  $\beta$ -Cyclodextrin, Inclusion complex, Atomic force microscopy, Fourier Transform Infra red , Thermal analysis, Molecular Docking

## 1. Introduction

Cyclodextrins (CDs) are cyclic oligosaccharides which have six, seven, and eight D-glucopyranose units for  $\alpha$ ,  $\beta$ , and  $\gamma$ -cyclodextrin respectively. They form inclusion complexes with guest molecules of suitable polarity and size [1-6], because of their special molecular structure with a hydrophobic central cavity and a hydrophilic outer surface. The difference in polarity within the molecule and the restricted space provided by cyclodextrin cavity significantly influences photo physical and photochemical processes of guest molecule.

Chalcones are used as therapeutic agents for cardiovascular diseases [7] and exhibit interesting biological properties [8-10]. They possess high photosensitivity, thermal stability and are used in developing various crystalline electro-optical devices [11]. It is well known that Dibenzalacetone [1,5-Diphenyl-1,4-pentadien-3-one] (DBA) is a component of sun screens because it is capable of absorbing UV light. It is also used as ligand in organometallic chemistry. Dibenzalacetone (DBA) is less fluorescent in aqueous solution, but its fluorescence intensity increases by the addition of  $\beta$ -Cyclodextrin ( $\beta$ -CD). Now-a-days inclusion complexation with  $\beta$ -CD is widely used in various fields such as medicine [12-15], chemistry [16,17], agriculture [18] etc. Ramamurthy, et al., [19,20] have exploited the use of CDs as host to examine photochemical and photo physical processes that occur in molecules complexed within them and to compare their behavior in aqueous solution and solid state. Earlier we reported spectro fluorometric study on inclusion complexation of 2-amino-6-fluorobenzothiazole [21], Benzisothiazole [22] and 3-amino-5-nitro benzisothiazole [23] with  $\beta$ -CD. In the present work we report inclusion complexation of DBA with  $\beta$ -CD in solution and solid state.

## 2. Experimental

### 2.1 Instruments

Absorption spectrum was recorded with a Hitachi model U-2001 spectrophotometer. Fluorescence measurements were made using a Jasco.FP-550 spectrofluorimeter. The isosbestic wavelengths were used as the  $\lambda_{\text{exi}}$  for measuring fluorescence intensities at any analytical wavelength. pH values were measured by using an Elico LI-105 model pH meter. Fluorescence lifetimes were determined using a time-correlated Pico second Photon counting Spectrofluorimeter (Tsunami, spectrophysics, USA). FT-IR Spectra were obtained with Avtar-330 FT-IR Spectrophotometer using KBr pellet. The spectra were recorded in the frequency range 4000-400  $\text{cm}^{-1}$ . Microscopic morphological (SEM) measurements were performed with JEOI-JSM 5610 LV. Surface morphology was also recorded using AGILENT-N 9410 A SERIES 5500 AFM. The samples were analyzed by DSC using a Mettler Toledo SR system. The samples (5gm each) were placed into pierced aluminum container which found use with hydrate and solvate loss as well as to relieve internal pressure in the case of ordinary sample. The studies were performed under static air atmosphere in the temperature range of 20 °C to 200 °C at a heating rate of 10 °C/min. The peak temperatures were determined after calibration with standard. The powder XRD patterns of DBA, physical mixture and the complex were recorded by using automated Philips Holland-PW 1710 scanner with filter Cu radiation over the interval 5-60°/2 $\theta$ . The operation data were as follows: voltage 35 KV, current 20 mA, filter Cu and scanning speed 1°/min.

### 2.2 Reagents

Dibenzalacetone (DBA) was synthesized by Aldol condensation reaction carried out between benzaldehyde and acetone in alkaline medium [24]. Then it was purified by repeated recrystallisation from ethanol.  $\beta$ -Cyclodextrin was purchased from S.D. fine chemicals and used as received. Triply distilled water was used for the preparation of experimental

solutions. pH solution (6.8) was prepared by using appropriate amounts of NaOH and H<sub>3</sub>PO<sub>4</sub>. The concentration of experimental solutions was in the order of 3×10<sup>-3</sup> mol/dm<sup>3</sup>. Solutions for UV study and fluorimetric titration were prepared just before taking measurements.

### 2.3 Preparation of Solid inclusion Complexes of DBA with β-CD

Solid DBA: β-CD complex was prepared using established standard co-precipitation method [21-23]. DBA and β-CD with 1:1 molar ratio were accurately weighed separately. Saturated β-CD solution was prepared in water. Then DBA solution in methanol was added to β-CD solution slowly till a suspension was formed. The suspension was stirred for 30 min at 40 °C and kept stirring at room temperature for 24 h. After getting clear solution (without any suspended particles) it was kept in lyophilizer for 24 hours. The precipitate obtained was filtered through 0.45 μm membrane filter and dried at 40° C in an oven for 24 h. The dried complex was ground to fine powder. Physical mixture of DBA: β-CD in 1:1 molar ratio was prepared by homogeneously blending previously sieved (63-160 μm) individual components in a mortar.

### 2.4 Job's continuous variation method

Determination of stoichiometry of the inclusion complex was provided by the continuous variation technique (Job's plot) based on the difference in absorbances, ΔOD (ΔOD=A<sub>0</sub>-A). of DBA observed in the presence of β-CD. Equimolar solutions of the DBA and the corresponding β-CD was prepared and mixed to standard volumes and proportions in order that the total concentration remained constant ( [DBA]<sub>t</sub> + [β-CD]<sub>t</sub> = Constant ) but the ratio of the initial concentrations varied between 0 and 1. ΔOD values in the preparation of guests were calculated by measuring the absorbance of DBA in the absence (A<sub>0</sub>) and presence (A) of the corresponding concentrations of β-CD. Also, an equimolar solution of β-CD was used as a blank, to take into account its refractive index.

## 2.5 Molecular Docking Study

The most probable structure of the DBA:  $\beta$ -CD inclusion complex was determined by molecular docking studies using the Patch Dock server [25]. The 3D structural data of  $\beta$ -CD and DBA was obtained from crystallographic databases. The guest molecule (DBA) was docked in to the host molecule ( $\beta$ -CD) cavity using Patch Dock server by submitting the 3D co-ordinate data of DBA and  $\beta$ -CD molecules. Docking was performed with complex type configuration settings. Patch Dock server followed a geometry-based molecular docking algorithm to find the docking transformations with good molecular shape complementarity. Patch Dock algorithm separated the Connolly dot surface representation [26, 27] of the molecules into concave, convex and flat patches. These divided complementary patches were matched in order to generate candidate transformations and evaluated by geometric fit and atomic desolvation energy scoring [28] function. RMSD (root mean square deviation) clustering was applied to the docked solutions to select the non-redundant results and to discard redundant docking structures.

## 3. Results and discussion

### 3.1 Interaction of DBA with $\beta$ -CD in solution

The absorption maxima, and fluorescence maximum of DBA at different concentrations of  $\beta$ -CD at pH 6.8 is given in Table 1. Upon increasing the concentration of  $\beta$ -CD, the absorption maxima at longer wavelength are blue shifted with a gradual decrease in their absorbance (Fig.1) up to the concentration ( $12 \times 10^{-3}$  M). This behavior has been attributed to the enhanced dissolution of the guest molecule by inclusion complexation [22] through the hydrophobic interaction between the guest molecule and  $\beta$ -CD.

The binding constant and stoichiometry of DBA:  $\beta$ -CD complex can be determined from the changes in absorbance of DBA by the addition of  $\beta$ -CD using

Benesi-Hildebrand equation [BH]. BH equations for 1:1 and 1:2 complex [29] are shown by eqns (1) and (2) respectively.

$$1/(A-A_0) = 1/\Delta\varepsilon + 1/K[DBA]_0 \Delta\varepsilon[\beta\text{-CD}]_0 \text{-----}(1)$$

$$1/(A-A_0) = 1/\Delta\varepsilon + 1/K[DBA]_0 \Delta\varepsilon[\beta\text{-CD}]_0^2 \text{-----}(2)$$

Where  $(A-A_0)$  is the difference between the absorbance of DBA, in the presence and absence of  $\beta$ -CD.  $\Delta\varepsilon$  is the difference between the molar extinction co-efficient of DBA in the presence and absence of  $\beta$ -CD.  $[DBA]_0$  and  $[\beta\text{-CD}]_0$  are the initial concentrations of DBA and  $\beta$ -CD, respectively. A good linear correlation ( $R^2 = 0.9919$ ) is obtained when  $1/(A-A_0)$  is plotted against  $1/[\beta\text{-CD}]$  [Fig.1.inset], whereas a non-linear plot is obtained when  $1/(A-A_0)$  is plotted against  $1/[\beta\text{-CD}]^2$ . This shows that the complex formed between DBA and  $\beta$ -CD has 1:1 stoichiometry. The binding constant value 'K' for 1:1 inclusion complex is determined from slope of the plot according to eqn (3) [30, 21-23] and it is found to be  $34 \pm 2 \text{ M}^{-1}$  at 303K

$$K = 1/ \text{Slope } [A'-A_0] \text{-----}(3)$$

Fig.2 represents the fluorescence spectra of DBA at pH 6.8 with different concentrations in aqueous solution of  $\beta$ -CD. The enhancement of fluorescence intensity of DBA (both the maximum) with increasing concentration of  $\beta$ -CD up to the concentration  $12 \times 10^{-3} \text{ M}$  suggests the formation of inclusion complex between DBA and  $\beta$ -CD. An increase in the fluorescence intensity of guest molecule with increasing the concentration of host during the formation of inclusion complex has been reported earlier [21, 31 and 32]. The  $\beta$ -CD dependence of DBA fluorescence can be analyzed by BH equations for 1:1 [21, 22] and 1:2 complex [33] using equations (4) and (5) respectively.

$$1/I-I_0 = 1/I'-I_0 + 1/K (I'-I_0)[\beta\text{-CD}] \text{-----} (4)$$

$$1/I-I_0 = 1/I'-I_0 + 1/K (I'-I_0)[\beta\text{-CD}]^2 \text{-----} (5)$$

Where 'K' is binding constant,  $I_0$  is the intensity of fluorescence of DBA without  $\beta$ -CD.  $I$  is the intensity of certain concentration of  $\beta$ -CD, and  $I'$  is the fluorescence intensity of DBA with the highest concentration of  $\beta$ -CD. A non-linear relation is observed when  $I/I_0$  is plotted against  $1/[\beta\text{-CD}]^2$ , but a linear plot is obtained for  $I/I_0$  Vs  $1/[\beta\text{-CD}]$  (Fig.2a inset). This shows that the complex formed between DBA and  $\beta$ -CD has 1:1 stoichiometry. From the slope of the 1:1 plot, the Binding constant 'K' calculated using the equation (6) is found to be  $51 \pm 2 \text{ M}^{-1}$  at 303 K.

$$K = 1/ \text{Slope } [I'-I_0] \text{ ----- (6)}$$

### 3.1.1 Jobs Plot

The stoichiometry of the inclusion complex DBA:  $\beta$ -CD is also confirmed by using Job's continuous variation method using the absorption data. Fig.2b shows the change in optical density ( $\Delta$ OD) against mole fraction of DBA. In this plot  $\Delta$ OD maximum at 0.5 which indicates the stoichiometry of the complex between DBA and  $\beta$ -CD is 1:1.

### 3.1.2 Analysis of fluorescence decay curve

The fluorescence lifetimes are often very sensitive indicators for exploring the local environment around the excited state fluorophore [34, 35]. With the above point of view to acquire a deep insight into the excited state photo physics of the guest and its alterations in  $\beta$ -CD confinement, we have recorded the fluorescence lifetimes of DBA in water and at different concentration of  $\beta$ -CD. The excitation wavelength was fixed at 320 nm and the emission wavelength was fixed at 340 nm. The fluorescence decay behaviors of DBA both in water and in  $\beta$ -CD environments are found to be quite different.

The lifetime and amplitudes of the decay of DBA with and without  $\beta$ -CD are given in Table.2. In water the fluorescence decay of DBA obtained from monitoring the emission at 340 nm is a single exponential with lifetime value 7.89 ns ( $\tau_1$ ). However in the presence of



various concentrations of  $\beta$ -CD, decay curves gave a best fit for the biexponential decay with lifetimes of  $\tau_1$  in the range of 7.64 ns to 0.1 ns and  $\tau_2$  in the range of 2.3 ns to 2.96 ns. Triple exponential analysis was also attempted, but  $\chi^2$  was not improved. On increasing the concentration of  $\beta$ -CD, the lifetime of the complex ( $\tau^2$ ) is higher and its amplitude is also increased. This is due to the formation of inclusion complex between DBA and  $\beta$ -CD (22, 23 and 36]. The  $\chi^2$  values for the single and double exponential fittings were less than 1.2. The observed enhancement in lifetime indicates that DBA molecule experiences less polar hydrophobic environments within the  $\beta$ -CD cavity resulting in the interaction of non-radioactive decay process. Further the increase in fluorescence lifetime is a result of the significant interaction of DBA with hydrophobic  $\beta$ -CD cavity.

The ratio of the pre-exponential factors ( $B_2/B_1$ ) is related to the concentration of the two components by the following eqn (7)

$$B_2/B_1 = C_2 K r \epsilon_2 / C_1 K r_1 \epsilon_1 \text{-----}(7)$$

Where  $C_1$ , is the concentration of DBA,  $Kr$  and  $\epsilon$  are the radioactive rate constant and the molar extinction co-efficient at the excitation wavelength respectively. The subscript 1 and 2 refer the free and complex of DBA with  $\beta$ -CD respectively. Since  $Kr$  is a constant and  $\epsilon_1 = \epsilon_2$ , Eqn (7) is simplified as  $B_2/B_1 = C_2/C_1$ . In excess of  $[\beta\text{-CD}]$  with respect to the DBA,  $B_2/B_1$  [37] can be written as Eqn (8).

$$B_2/B_1 = K [\beta\text{-CD}] \text{-----}(8)$$

Fig.2c shows the plot of  $B_2/B_1$  Vs  $[\beta\text{-CD}]$ . The linearity in the plot with the correlation coefficient of 0.9947 reflects the formation of 1:1 complex between DBA and  $\beta$ -CD. The binding constant  $K$  calculated for this complex is  $51 \pm 2 \text{ M}^{-1}$  at 303 K.

### 3.1.3 Spontaneity of inclusion complexation reaction

The Gibbs free energy change ( $\Delta G$ ) for this inclusion process was determined from the binding constant value using the following equation at 303K [21-23, 30]

$$\Delta G = - RT \ln K \quad \text{----- (9)}$$

Where  $\Delta G$  is the Gibbs free energy change,  $R$  is the gas constant [J/mol.K]  $T$  is the temperature in Kelvin and “ $K$ ” is the binding constant in  $\text{mol}^{-1}$ . When the “ $K$ ” value from absorption data is used in the equation (9), it gives the  $\Delta G$  values  $-8.9 \text{ KJ mol}^{-1}$  and the “ $K$ ” value from fluorescence data, it is  $-9.8 \text{ KJ mol}^{-1}$ .

The negative values indicate that inclusion complexation reaction proceeded spontaneously at 303 K.

## 3.2 Interaction of DBA with $\beta$ -CD in Solid state

### 3.2.1 FT-IR Spectral analysis

The solid inclusion complex prepared by co-precipitation method is analyzed by FT-IR spectroscopy. The FT-IR spectra of  $\beta$ -CD, pure DBA, physical mixture of DBA and  $\beta$ -CD and solid complex of DBA with  $\beta$ -CD are shown in Fig.3. When the guest molecule is encapsulated by means of inclusion complexation reaction, the absorption bands resulted from the included part of guest molecule are generally shifted in their position or intensity may be altered [37]. If  $\beta$ -CD and DBA form a solid inclusion complex, the non-covalent interactions between  $\beta$ -CD and DBA such as hydrophobic interactions, van der Waals interactions and hydrogen bonding lower the energy of the included part of DBA, thus reducing the absorption intensities of the corresponding bands. The O-H stretching frequency appears  $3361 \text{ cm}^{-1}$  in  $\beta$ -CD, it appears at  $3369 \text{ cm}^{-1}$  in physical mixture. It is shifted to  $3408 \text{ cm}^{-1}$  with reduced intensity in the case of solid inclusion complex. Slight shifts are observed in C-H, C=O stretching frequencies of DBA and solid inclusion complex. The aromatic ring C-C stretching

vibrations appear at  $1591\text{ cm}^{-1}$  and  $1493\text{ cm}^{-1}$  in DBA. It is shifted to  $1593\text{ cm}^{-1}$  and  $1494\text{ cm}^{-1}$  in solid inclusion complex with considerable reduction in the intensity of the peak. Similarly ring C-H bending vibration of DBA appeared at  $759\text{ cm}^{-1}$  and  $595\text{ cm}^{-1}$  shifted to  $760.7\text{ cm}^{-1}$  and  $570\text{ cm}^{-1}$  in the case of solid inclusion complex with slight reduction in peak intensity. These changes occur when the benzene ring of DBA is entrapped into the nano hydrophobic cavity of  $\beta$ -CD [30]. There is no appreciable change in the stretching frequencies of physical mixture. These observations clearly indicate the formation of inclusion complex between DBA and  $\beta$ -CD.

### 3.2.2 SEM image analysis

The surface morphology of  $\beta$ -CD, DBA, Physical mixture and solid inclusion complex of  $\beta$ -CD : DBA were examined by Scanning Electron Microscopy [38]. SEM images of  $\beta$ -CD, DBA, Physical Mixture and inclusion complex of DBA:  $\beta$ -CD are shown in Fig.4. In  $\beta$ -CD, the particles are quite dense and well separated from each other whereas in DBA the particles are aggregated and are loosely bounded to each other. The physical mixture of both the components (Fig.4c) exhibited the characteristics of both DBA and cyclodextrin particles. However the DBA:  $\beta$ -CD inclusion complex (Fig.4d) appears as a compact and homogeneous plate like structure with a drastic change in the morphology and shape of the particles. It is no longer possible to differentiate DBA and  $\beta$ -CD in the complex which confirms the interaction between DBA and  $\beta$ -CD during the formation of inclusion complex [39].

### 3.2.3 XRD analysis

Evidence for the inclusion complexation of DBA with  $\beta$ -CD is also obtained from Powder XRD. It is a useful method for the detection of CD encapsulation and it has been used to assess the degree of crystallinity of the given sample. Generally the crystalline nature of the guest molecule is reduced and more number of amorphous structures are increased in the solid inclusion complex [40,41]. Hence the solid complexes usually exhibit less numbered as well as

less intense peaks. This shows that overall crystallinity of complex is decreased and the solubility is increased due to its amorphous nature.

DBA exhibits characteristic peaks at  $2\theta$  values of  $12.93^\circ$ ,  $18.99^\circ$ ,  $19.31^\circ$ ,  $19.68^\circ$ ,  $20.28^\circ$ ,  $24.75^\circ$ , and  $27.68^\circ$  [ Fig 5b]. Most of the characteristic peaks of DBA are present in the diffraction pattern of physical mixture without loss of intensity [Fig.5c]. The diffraction pattern of  $\beta$ -CD exhibited important peaks at  $2\theta$  values of  $8.95^\circ$ ,  $10.56^\circ$ ,  $12.45^\circ$ ,  $18.60^\circ$ ,  $22.4^\circ$ ,  $31.8^\circ$ , and  $35.01^\circ$  [Fig.5a]. The X-ray diffraction pattern of the solid inclusion complex [Fig.5d] is evidently different from that of DBA,  $\beta$ CD, and physical mixture, because the inclusion complex formed between DBA and  $\beta$ -CD is semi crystalline in nature. The peak intensity of DBA at  $12.61^\circ$ ,  $19.47^\circ$ ,  $20.10^\circ$ , and  $24.59^\circ$  are reduced significantly in diffraction pattern of complex which suggested the reduction in crystallinity [Fig.5d]. Some low intensity peaks of DBA at  $27.68^\circ$ ,  $28.16^\circ$ ,  $29.60^\circ$  and  $29.92^\circ$  were absent after complexation with  $\beta$ -CD. This different pattern might be due to inclusion of DBA molecule into the cavity of  $\beta$ -CD. Further, appearance of new low intense peaks at  $2\theta$  values for the patterns of DBA/  $\beta$ -CD ( $32.19^\circ$  and  $33.19^\circ$ ) inclusion complex indicates the change in DBA and CD environment after inclusion complexation.

### 3.2.4 DSC analysis

DSC represents an effective and inexpensive analytical tool widely used for a rapid preliminary qualitative investigation of thermal behavior of the inclusion complexes prepared by co-precipitation method [42]. When guest molecule is included in  $\beta$ -CD cavity or crystal lattice their melting and sublimation points may shift to different temperature or disappear [43]. DSC curve of pure  $\beta$ -CD [fig.6a] shows an endothermic peak at  $118^\circ\text{C}$ , TG of  $\beta$ -CD shows a weight loss about 15 %. It could be due to the guest water molecules present in  $\beta$ -CD cavity. There is no significant mass loss in TG up to  $270^\circ\text{C}$  whereas above this temperature decomposition of  $\beta$ -CD is started. The thermo gram of DBA [fig.6b] shows an endothermic peak at  $114^\circ\text{C}$  due to its phase transition. In the thermo gram of DBA : $\beta$ -CD complex [fig.6d], the endothermic peak is found at  $108^\circ\text{C}$ , there is no weight loss in the TG curves of DBA and

DBA :  $\beta$ -CD solid inclusion complex. It shows clearly that they are free from hydrated water molecules. It is also confirmed by determining the melting point of DBA and solid inclusion complex is 113 °C and 108 °C respectively using Sigma melting point apparatus. The lower melting point of inclusion complex is due to melting point depression by the  $\beta$ -CD [44], similar observation was found when felodipine and carbamazepine were complexed with  $\beta$ -CD, the endothermic temperature of inclusion complex was lowered by 3 and 5 °C respectively [44,45]. Physical mixture of  $\beta$ -CD and DBA, shows the weight loss nearly from 80-120 °C in TG [fig.6c] which is due to presence of water molecules in  $\beta$ -CD cavity and the endothermic peak at 113 °C is due to the melting point of DBA. The difference in thermal behavior between inclusion complex and host ( $\beta$ -CD) clearly reveals encapsulation of DBA in  $\beta$ -CD cavity.

### 3.2.5 AFM Analysis

AFM studies are used to visualize the surface texture of the deposited films, especially when the surface texture sizes are less than 3 micron [46]. The film is prepared by re-suspending the compound and complex in methanol, followed by dilute dispersion on freshly cleaved mica and then by thorough drying the particles are fixed on to the surface. AFM analysis is quite ideal for measuring the nanometric dimensional surface roughness and for visualizing the surface nanotexture of the deposited film. Visualization of surface topography of the guest (DBA) and the complex using AFM analysis is given in Fig.7. The peak to valley distance in these images is used as an indicator of the surface roughness. When the distance between the peak and the valley is more which means that it has a rougher surface and if the distance is less it indicates the smoothness of surface [47]. Based on this peak and valley distance, the AFM image of pure DBA (Fig.7a) shows a rough surface and uneven distribution. But in the case of solid complex the rough surface of DBA is changed into a smooth surface. The changes in surface morphology and the modification of the crystals may be taken as a proof for the interaction of DBA with  $\beta$ -CD (Fig.7b) (43).

### 3.3 Analysis using MOPAC software

The structure of the inclusion complex is established using MOPAC/AM1 software. The calculations show the total length of DBA molecule is found to be 13.34 Å (Table 3). The cavity length of  $\beta$ -CD is 7.8 Å, the inner diameter of  $\beta$ -CD cavity in the narrow edge and wide edge are 5.6 Å and 6.8 Å respectively [30, 48]. According to the size matching rule [49] only a portion of DBA molecule could be entrapped in to  $\beta$ -CD cavity. The low value of Binding constant 'K' reveals the possibility of only partial accommodation [22] of DBA in  $\beta$ -CD cavity. 'K' value is an important parameter to characterize the interaction between guest and host molecule and also reflects the intensity of binding force between them [22]. Based on these results the structure of solid inclusion complex is proposed.

### Molecular docking study of inclusion process

The 3D structure of  $\beta$ -CD and DBA obtained from crystallographic databases are shown in Figs. 8a and 8b. The guest molecule, DBA was docked into the cavity of  $\beta$ -CD using Patch Dock server. The Patch Dock server program provides several possible docked models for the most probable structure based on the energetic parameters such as geometric shape complementarity score [50], approximate interface area size and atomic contact energy [28] of the DBA: $\beta$ -CD inclusion complex [Table.4]. The docked DBA:  $\beta$ -CD 1:1 model (Fig. 8c) with the highest geometric shape complementarity score 3218, approximate interface area size of the complex 411.4 Å<sup>2</sup> and atomic contact energy -265.9 kcal/mol was the highly probable and energetically favorable model and it is in good correlation with results obtained through experimental methods.

## 4. Conclusions

The following conclusions have arrived on the basis of the above results.

- i. Using Benesi- Hildebrand plot and Job's continuous variation method, the stoichiometry of the DBA:  $\beta$ -CD inclusion complex is found to be 1:1.
- ii. Time - resolved fluorescence spectral study in aqueous solutions shows the presence of two species namely free DBA and DBA:  $\beta$ -CD inclusion complex.
- iii. The solid complex prepared by co-precipitation method is characterized by UV-Visible, FT-IR, DSC, XRD and microscopic morphological image analysis using SEM and AFM.

Based on these findings, the interaction between DBA and  $\beta$ -CD is confirmed and the structure of 1:1 inclusion complex, DBA: $\beta$ -CD<sub>x</sub> is proposed. The Docking study suggests that the proposed structure is found to be highly probable and energetically favorable model.

## References

- [1] D.Duchene (editor), Cyclodextrins and their Industrial Uses, Editions de Sante, Paris. 1987.
- [2] A. Munoz de la Pena, T.T. Ndou, J.B. Zung, K.L. Greene, D.H. Live, I.M. Warner, J. Am. chem. Soc. 113 (1991) 1572.
- [3] A. Munoz de la Pena, I. Duran-meras, F. Salinas, I.M. Warner, T.T. Ndou, Anal. Chim. Acta. 255 (1991) 351.
- [4] S. Scypinski, L.J. Cline Love, Anal. Chem. 56 (1984) 331.
- [5] J Szejtli, Cyclodextrin and their Inclusion Complexes, Akademiai Kiado, Budapest. 1982.
- [6] J. Szejtli, T.Osa. (editors). Comprehensive supramolecular Chemistry, Elsevier Science Ltd,

Oxford (U.K) .1996.

- [7] S. Shibata, *Stem Cells*. 12 (1994) 44.
- [8] A. Phrutivorapongkul, V.Lipipun, N.Ruangrungsi, K.Kirtikara, K.Nishikawa, S.Maruyama, T.Watanabe, T.Ishikawa, *Chem. Pharm. Bull.* 51 (2003) 187.
- [9] S.Pandey, S.N. Suryawuanshi, S.Gupta, V.M.L.Srivastra, *Eur.J.Med. Che.* 40 (2005) 751.
- [10] S.Gafner, J.L.Wolfender, S.Mavi, K.Hostettmann, *Planta Medica* 03 (1996) 62.
- [11] Y.Goto, M.Nakayama, *Jpn. J. Appl. Phys.* 27 (1988) L429.
- [12] C. Yanez, R.Salazar, L.J. Nunez-vergara, J. A. Squella, *J.Pharmaceut. Biomed. Anal.* 35 (2004) 51.
- [13] S. Rawat, S.K. Jain, *Euro J Pharm and Biopharm.* 57 (2004) 263.
- [14] J.J. Berzas, A.Alanon, J.A. Lazaro, *Talanta.* 58 (2002) 301.
- [15] S.O. Fakayode, I.M. Swamidoss, M.A. Busch, Kw.Busch, *Talanta.* 65 (2005) 838.
- [16] O.Csernak, A. Buvvari-Barcza, L. Barcza, *Talanta.* 69 (2006) 425.
- [17] G.Zhang, S. Shuang, C. Dong, J. Pan, *Spectrochim. Acta Part A* .59 (2003) 2935.
- [18] N.L. Pacioni, A.V. Veglia, *Anal. Chim. Acta.* 488 (2003) 193.
- [19]. V. Ramamurthy, D.F. Eaton, *Acc. Chem. Res.* 21 (1988) 300.
- [20] M.S. Syamala, V. Ramamurthy, *Tetrahedron* 44 (1988) 7223.
- [21] R.Rajamohan, S. Kothainayaki, M. Swaminathan, *Collect. Czech. Chem. Commun.* 73 (2008) 147.
- [22] R.Rajamohan, S. Kothainayaki, M. Swaminathan, *J Fluoresc.* 21 (2011) 521.



- [23] R.Rajamohan, S. Kothainayaki, M. Swaminathan, *Spectrochim Acta Part A*, 69 (2008) 371.
- [24] Al.Vogel, *Practical Organic Chemistry*, V edition, (1989) 1033.
- [25] Dina Schneidman-Duhovny, Yuval Inbar, Ruth Nussinov, Haim J. Wolfson, PatchDock and SymmDock: servers for rigid and symmetric docking, *Nucl. Acids Res.*, 33 (2005) 363.
- [26] M.L. Connolly, Solvent-Accessible Surfaces of Proteins and Nucleic Acids, *Science*, 221 (1983) 709.
- [27] M.L. Connolly, Analytical molecular surface calculation, *J. Appl. Crystallogr.*, 16 (1983) 548.
- [28] C. Zhang, G. Vasmatzis, J.L. Cornette, C. DeLisi, *J Mol Biol*, 267 (1997) 707.
- [29] H.A. Benesi, J.H. Hildebrand, *J.Am.chem.Soc.* 71 (1949) 2703..
- [30] K. Srinivasan, T.Stalin, K. Sivakumar, *Spectrochimica Acta Part A*, 94 (2012) 89.
- [31] M. Hoshino , M. Imamura , K. Ikehara , Y. Hama , *J.Phys. Chem.* 85 (1981) 1820.
- [32] K.A.Al Hassan , V.K. Klein, A.Sawaiyan , *Chem. Lett.* 212 (1993) 581.
- [33] S.K.Das, *Chemical physics letters*, 361 (2002) 21
- [34] J.R. Lakowicz, *Principles of Fluorescence Spectroscopy*, Plenum press, New York, (1986)
- [35] B.K. Paul, A. Samanta, N. Guchhait, *Langmuir* 26 (2010) 3214.
- [36] (a) M.A. El-Kemary, H.S. El-Gezawy, H.Y. El-Baradie, R.M. Issa, *Spectrochim Acta A Mol Biomol Spectrosc.* 58 (2002) 493.
- (b) M.A. El-Kemary, H.S. El-Gezawy, *J. Photochem.Photobiol. A*, 155 (2003) 151.

- (c) V.K.Indirapriyadharshini, P. Karunanithi, P. Ramamurthy, *Langmuir*, 17 (2001) 4056.
- (d) R. Rajamohan, M. Swaminathan, *Spectrochimica Acta Part A*, 83 (2011) 207.
- [37] J. Szejtli, T.osa, editors. vol 3, Pergamon press, Oxford, (1996) 253
- [38] H.Y. Wanrg, J.H.X. Guang Ferg. Y.I. Pang, *Spectrochimica Acta Part A*, 65 (2006) 100.
- [39] Li-Juan Yang, Shui-Xian Ma, Shu-Ya Zhou, Wen Chen, Ming-Wei Yuan, Yan-Qing Yin, Xiao-Dong Yang, *Carbohydrate Polymers* 98 (2013) 861.
- [40] E.E.M. Eid, A.B. Abdul, F.E.O. Suliman, M.A. Sukari, A.Rasedee and S.S. Fatah, *Carbohydrate Polymers*, 83 (2011) 1707.
- [41] J.Wang, Y.. Cao, B. Sun, C. Wang, *Food Chemistry*, 127 (2011) 1680.
- [42] I. Kacso, G.H. Borodi, S.I. Farcas, A. Hernanz and I. Bratu, *Journal of Inclusion Phenomena and Macrocyclic chemistry* 68 (2010) 175.
- [43] Hazuki Nerome, Siti machmidah, Wahyudiono, Ryuichi Fukuzato, Takuma Higashiura, Yong-Suk Youn, Youn-Woo Lee, Motonobu Goto, *The Journal of Supercritical Fluids* 83 (2013) 97.
- [44] J. Mielcarek, *J. Inclusion Phenom. Mol.* 30 (1998)243.
- [45] A. Cvetkovskii, R. Bettini, Lj. Tasic, M. Stupar, I. Casini, A.Rossi, F. Giordano, *J. Therm. Anal. Calorim.* 68 (2002) 669.
- [46] K. Sivakumar, T. Stallin, *Spectrochimica Acta Part A*, 79 (2011) 169.
- [47] Zoheb Karim and Rohana Adnan, *Archives of Environmental Science*, 6 (2012) 1.
- [48] J. Szejtli, *Cyclodextrin technology*, Kluwer, Academic Publisher , Dordecht (1988) 450.
- [49] Y.Liu, Y. Chen, B.Li, T. Wada, Y. Inoue, *Chemistry A, European Journal* 7 (2007) 2528.
- [50] D.Duhovny, R.Nussinov, H.J. Wolfson, Efficient Unbound Docking of Rigid Molecules. In Gusfield et al., Ed. *Proceedings of the 2'nd Workshop on Algorithms in*

Bioinformatics(WABI), Rome, Italy, Lecture Notes in Computer Science, 2452,  
Springer Verlag, (2002) 185.

### Figure captions:

1. **Fig. 1.** Absorption spectra of DBA with increasing concentration of  $\beta$ CD (1. Without, 2. 0.002, 3. 0.004, 4. 0.006, 5. 0.008, 6. 0.010 and 7. 0.012 M  $\beta$ CD). (1. **Inset** : Benesi-Hildebrand absorption plot of DBA with  $\beta$ CD ( $\lambda_{\text{abs}} = 230$  nm) (
2. **Fig. 2.** (a) Fluorescence spectra of DBA with increasing concentration of  $\beta$ CD (1. Without, 2. 0.002, 3. 0.004, 4. 0.006, 5. 0.008, 6. 0.010 and 7. 0.012 M  $\beta$ CDx), (b) **Inset** Benesi-Hildebrand fluorescence plot of DBA with  $\beta$ CD ( $\lambda_{\text{emi}} = 361$  nm), (b) Job's plot of DBA with  $\beta$ CD ( $\lambda_{\text{abs}} = 240$  nm). C). Plot of  $[\beta\text{-CD}]$  vs  $B_2/B_1$
3. **Fig. 3.** FT-IR spectra of a)  $\beta$ -CD b) DBA, c) physical mixture of DBA with  $\beta$ CD and d) solid complex of DBA with  $\beta$ CD.
4. **Fig. 4.** . SEM images of a)  $\beta$ -CD ( $\times 500$ ), b) DBA ( $\times 500$ ), b) physical mixture of DBA with  $\beta$ CD ( $\times 500$ ) and c) Solid complex of DBA with  $\beta$ CD ( $\times 500$ ).
5. **Fig. 5.** XRD patterns of a)  $\beta$ CD b) DBA, c) physical mixture of DBA with  $\beta$ CD and c) solid complex of DBA with  $\beta$ CD.
- 6 **Fig. 6.** Thermo gram [TG-DSC] of a) $\beta$ -CD b) DBA, c) physical mixture of DBA with  $\beta$ -CD and d) solid complex of DBA with  $\beta$ CD.
- 7 **Fig. 7.** Atomic force microscope 2D and 3D images of (a) DBA and (b) solid complex of DBA with  $\beta$ CD.
- 8 **Fig 8.** Ball and stick representation of (a)  $\beta$ -CD (b) DBA (c) 1:1 inclusion complex; the oxygen atoms are shown as red, carbon atoms are shown as golden balls and sticks,

and hydrogen atoms are not shown.

**Table. 1** The absorption and fluorescence spectral maxima of DBA in different concentration of  $\beta$ -CD at pH 6.8

Concentrations of $\beta$ -CD (mol dm <sup>-3</sup> )	pH 6.8					
	$\lambda_{\max}$ nm	abs	$\lambda_{\max}$ nm	abs	$\lambda_{\text{flu}}$ nm	$\lambda_{\text{flu}}$ nm
0	228.5	0.322	323.5	0.484	364	437
$2 \times 10^{-3}$	230.5	0.332	321.5	0.444	363	436
$4 \times 10^{-3}$	230.5	0.346	321.0	0.381	363	436
$6 \times 10^{-3}$	231.0	0.357	321.0	0.372	362	435
$8 \times 10^{-3}$	231.5	0.388	314.5	0.376	362	435
$10 \times 10^{-3}$	231.5	0.405	315.5	0.376	361	435
$12 \times 10^{-3}$	232.0 255.0	0.467 0.512	shoulder	shoulder	361	434

**Table 2.** Fluorescence lifetime and amplitude of DBA with increasing concentrations of  $\beta$ -CD (Excitation wavelength 320 nm, detection wavelength 340nm)

Concentration of $\beta$ -CD (M)	Lifetime	Relative amplitude	$\chi^2$	Standard deviation
0	$7.89 \times 10^{-9}$	100	1.103	$2.367 \times 10^{-9}$
0.002	$7.64 \times 10^{-9}$	60.43	1.011	$2.16 \times 10^{-10}$
	$2.3 \times 10^{-9}$	39.57		$1.25 \times 10^{-10}$
0.004	$7.39 \times 10^{-9}$	49.13	1.018	$3.61 \times 10^{-10}$
	$2.34 \times 10^{-9}$	50.87		$1.35 \times 10^{-10}$
0.006	$1.26 \times 10^{-10}$	56.55	1.187	$8.16 \times 10^{-10}$
	$2.42 \times 10^{-9}$	43.45		$1.35 \times 10^{-10}$
0.008	$1.14 \times 10^{-10}$	33.31	0.966	$3.42 \times 10^{-10}$
	$2.63 \times 10^{-9}$	66.69		$9.50 \times 10^{-11}$
0.010	$1.04 \times 10^{-10}$	26.43	0.959	$1.46 \times 10^{-9}$
	$2.74 \times 10^{-9}$	73.57		$1.30 \times 10^{-9}$
0.012	$1.00 \times 10^{-10}$	19.81	1.150	$8.20 \times 10^{-10}$
	$2.96 \times 10^{-9}$	80.19		$1.21 \times 10^{-10}$

**Table 3.** Bond length between various atoms of DBA

Atom	Bond distance (Å)
H <sub>28</sub> - H <sub>20</sub>	13.34
H <sub>28</sub> .C <sub>2</sub>	7.72
C <sub>8</sub> - C <sub>4</sub>	6.73
C <sub>8</sub> - H <sub>20</sub>	12.12
C <sub>9</sub> - H <sub>20</sub>	12.31
C <sub>9</sub> .C <sub>4</sub>	7.28
H <sub>19</sub> .C <sub>2</sub>	7.10
H <sub>29</sub> .C <sub>4</sub>	7.51

**Table 4:** Scores of the top 10 docked models of DBA:β-CD inclusion complex computed using Patch Dock server.

Model	Geometric shape complementarity score	Approximate interface area size of the complex Å <sup>2</sup>	Atomic contact energy kcal/mol
1	3218	411.4	- 265.9
2	2934	355.4	-255.5
3	2870	343.3	-252.8
4	2852	340.1	-243.2
5	2846	339.2	-239.1
6	2816	340.4	-243.5
7	2808	334.5	-235.8
8	2792	300.5	-213.6
9	2778	334.6	-241.3
10	2772	341.3	-246.0

Figures:

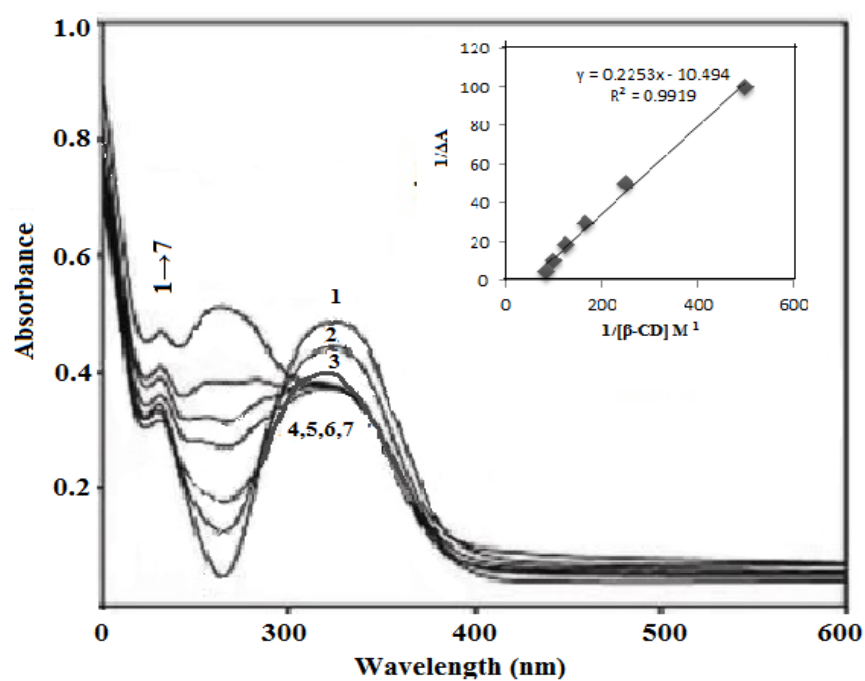


**Fig. 1.** Absorption spectra of DBA with increasing concentrations of  $\beta$ CD

(1. Without, 2. 0.002, 3. 0.004, 4. 0.006, 5. 0.008, 6. 0.010 and 7. 0.012 M  $\beta$ CD).

(Inset: Benesi-Hildebrand absorption plot of DBA with  $\beta$ CD ( $\lambda_{\text{abs}} = 230$  nm))



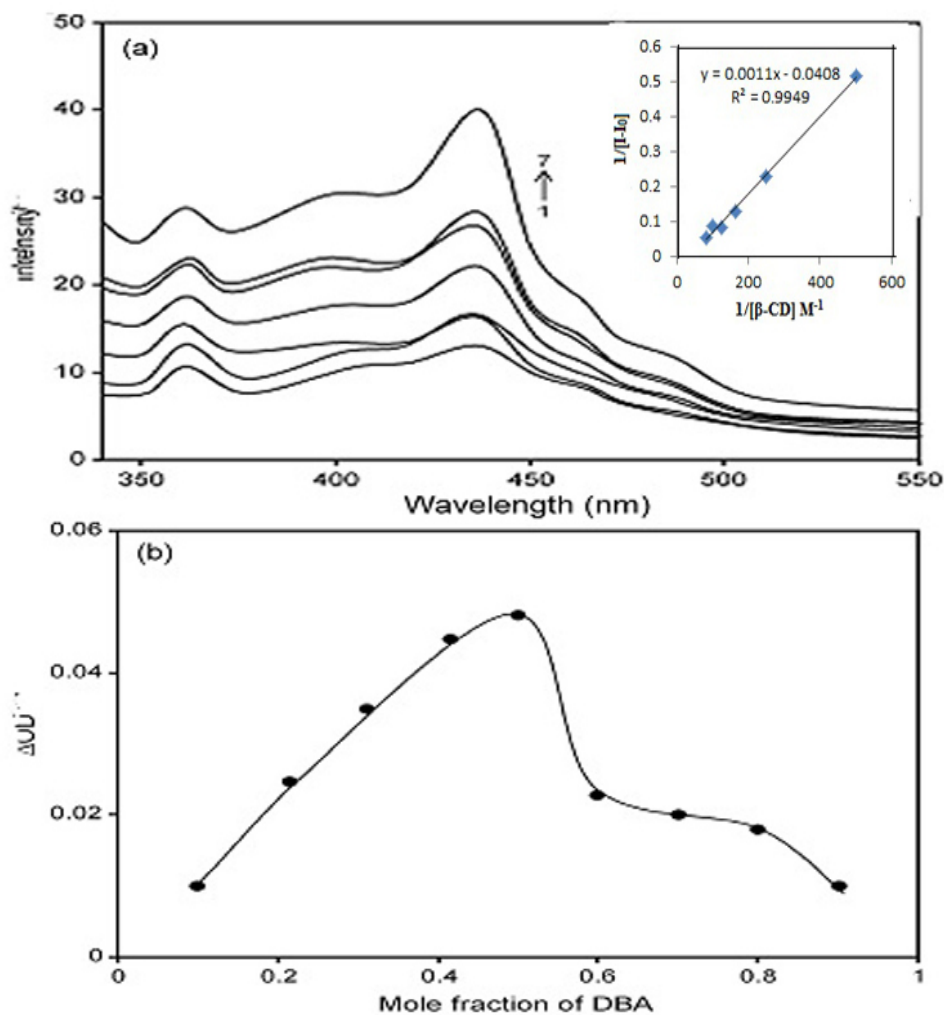


**Fig. 2.** (a) Fluorescence spectra of DBA with increasing concentrations of  $\beta$ CD (1. Without, 2. 0.002, 3. 0.004, 4. 0.006, 5. 0.008, 6. 0.010 and 7. 0.012 M  $\beta$ CD), (Inset : Benesi-Hildebrand fluorescence plot of DBA with  $\beta$ CD ( $\lambda_{\text{emi}} = 361 \text{ nm}$ ), (b) Job's plot of DBA with  $\beta$ CD ( $\lambda_{\text{abs}} = 230 \text{ nm}$ ).

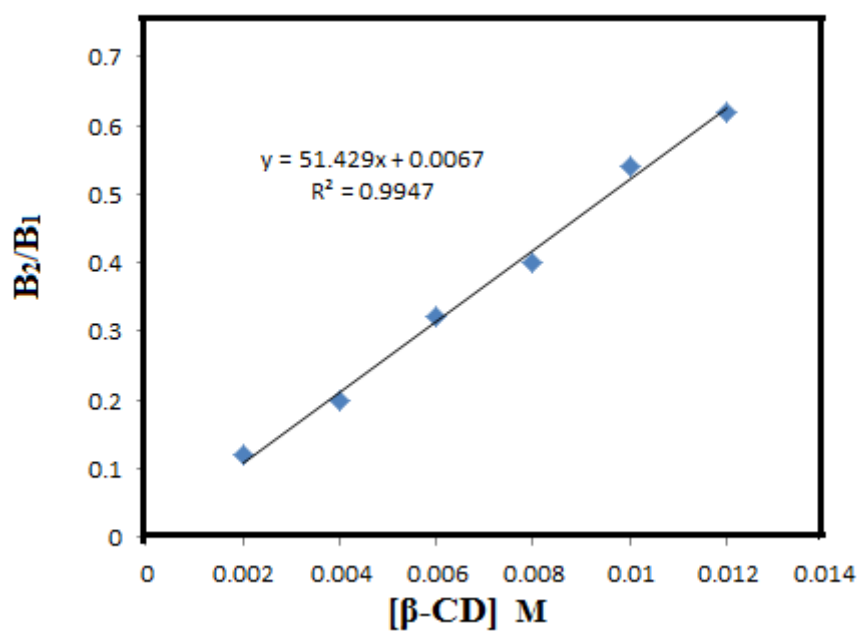
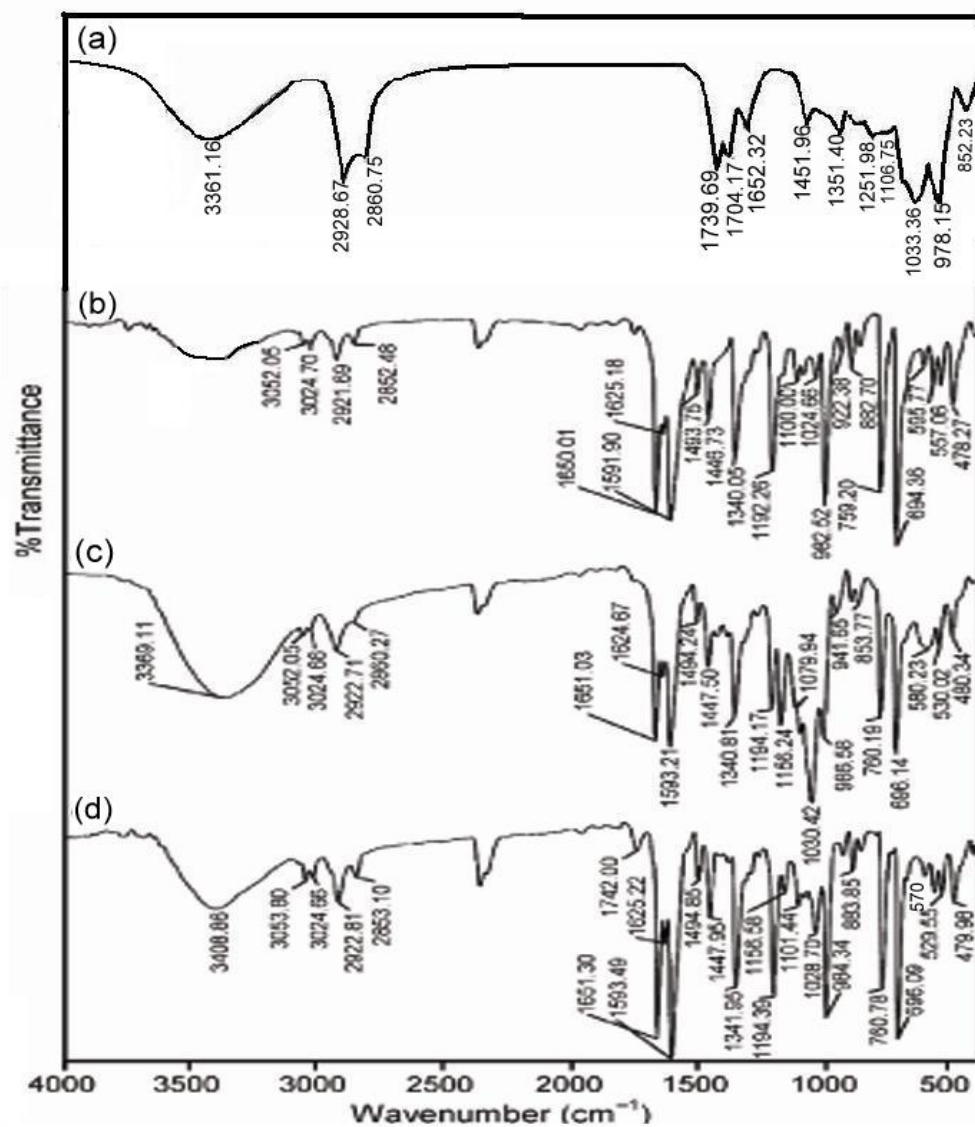
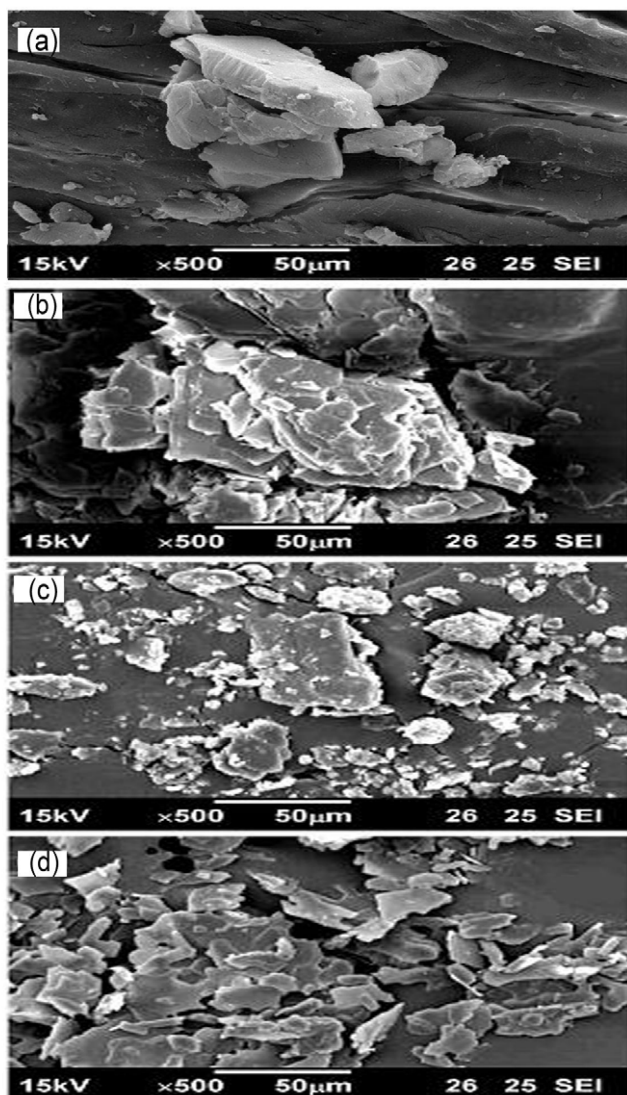


Fig.2c: Plot of [β-CD] vs B<sub>2</sub>/B<sub>1</sub>



**Fig. 3.** FT-IR spectra of a)  $\beta$ -CD b) DBA, c) physical mixture of DBA with  $\beta$ CD and d) solid compound DBA with  $\beta$ CD.



**Fig. 4.** SEM images of a)  $\beta$ -CD ( $\times 500$ ), b) DBA ( $\times 500$ ), c) physical mixture of DBA with  $\beta$ CD ( $\times 500$ ) and d) Solid complex of DBA with  $\beta$ CD ( $\times 500$ ).

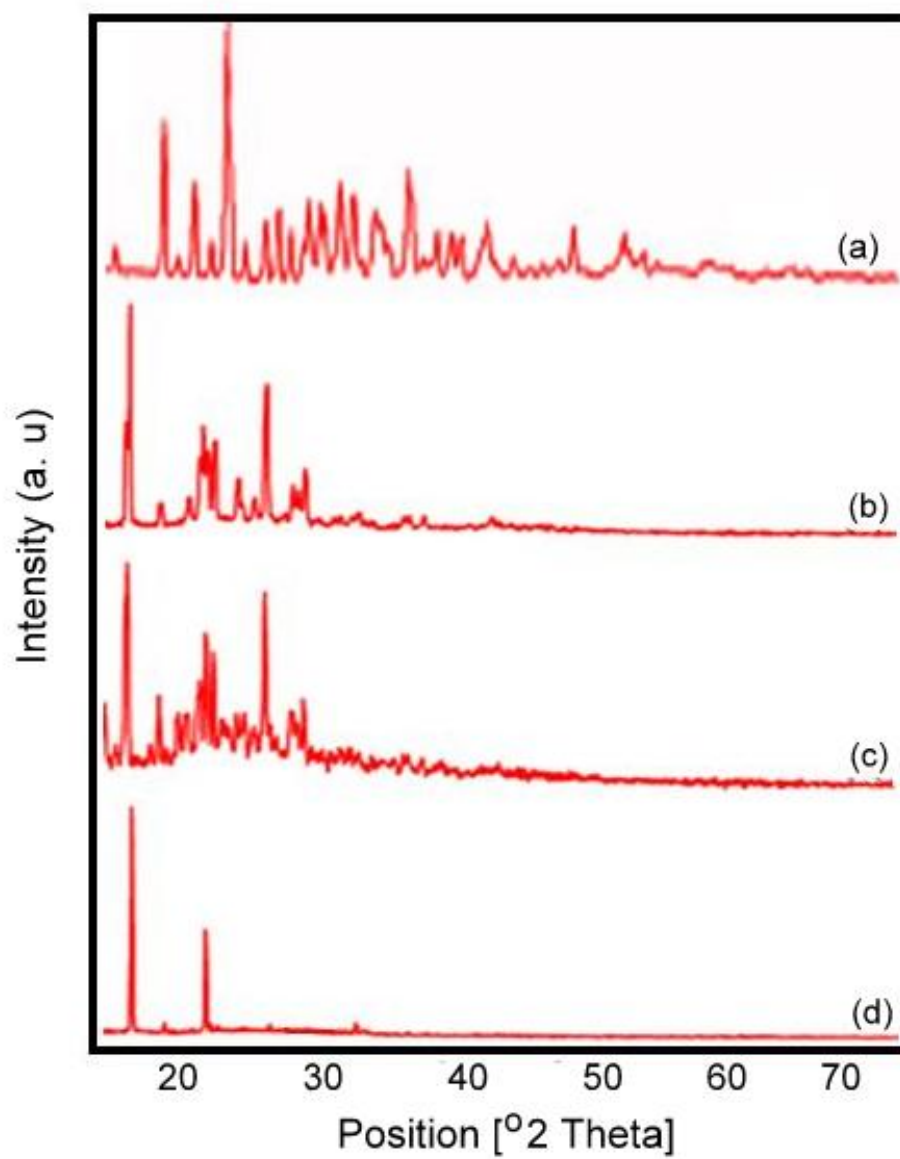


**Fig. 5.** XRD patterns of a)  $\beta$ CD b) DBA, c) physical mixture of DBA with  $\beta$ CD and d) solid complex of DBA with  $\beta$ CD.

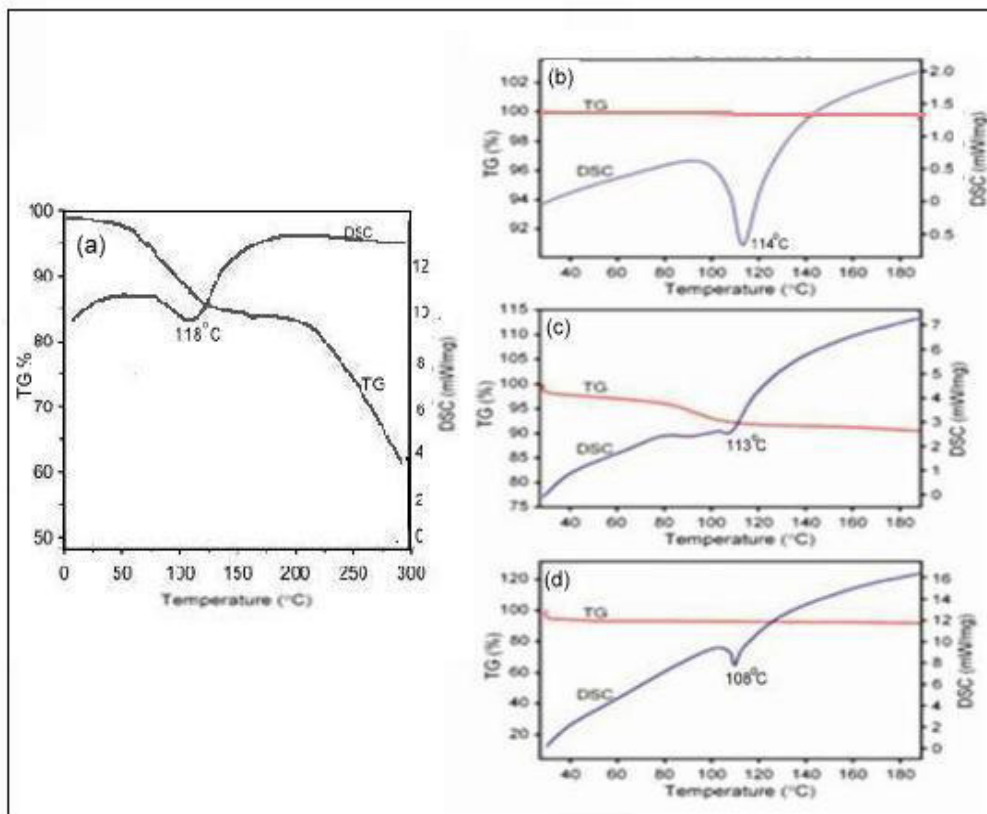


**Fig. 6.** Thermogram [TG-DSC] of a)  $\beta$ -CD b) DBA, c) physical mixture of DBA with  $\beta$ CDx and d) solid complex of DBA with  $\beta$ CDx.

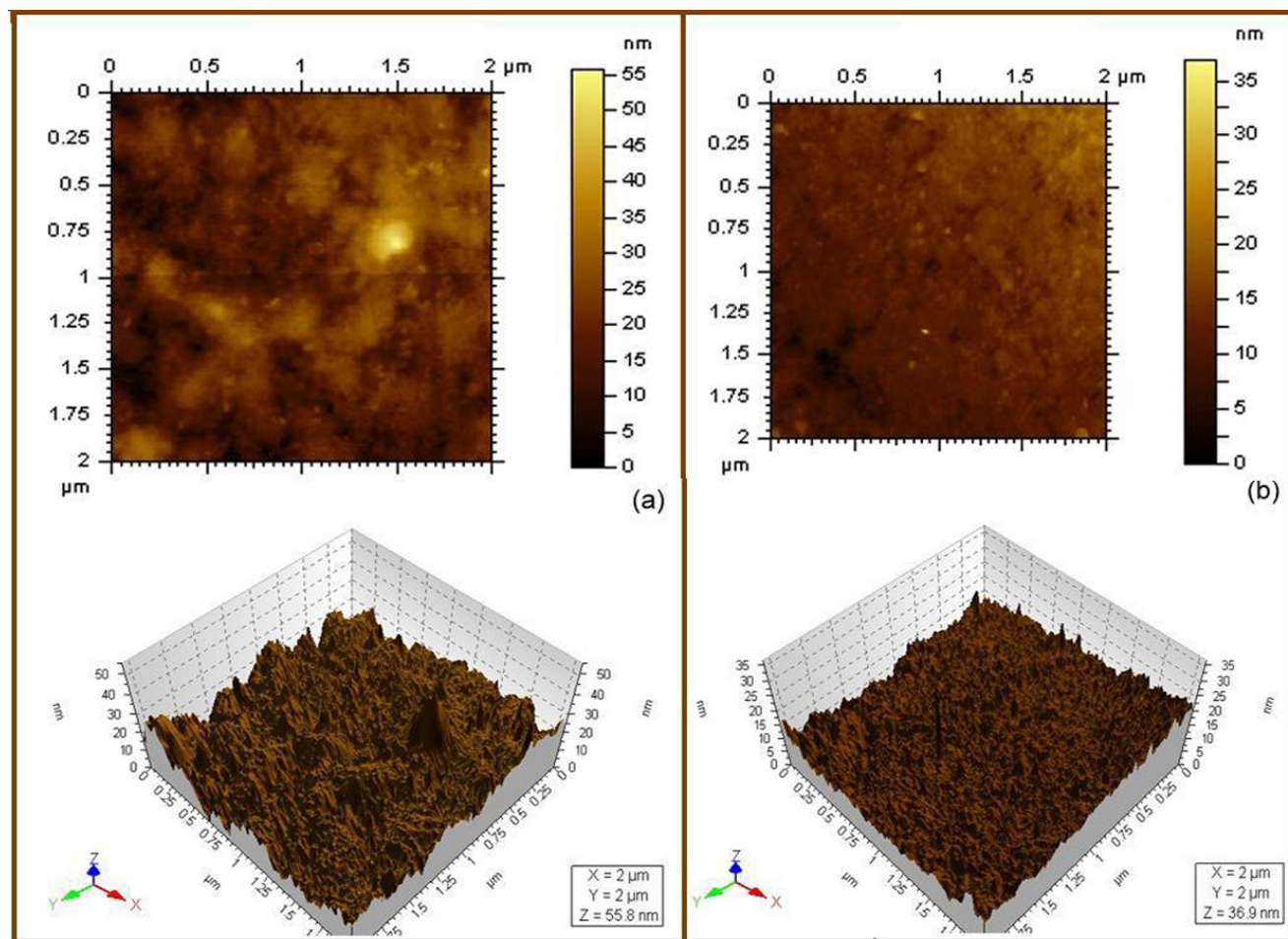


**Fig. 7.** Atomic force microscope 2D and 3D images of (a) DBA and (b) solid complex of DBA with  $\beta$ CD.



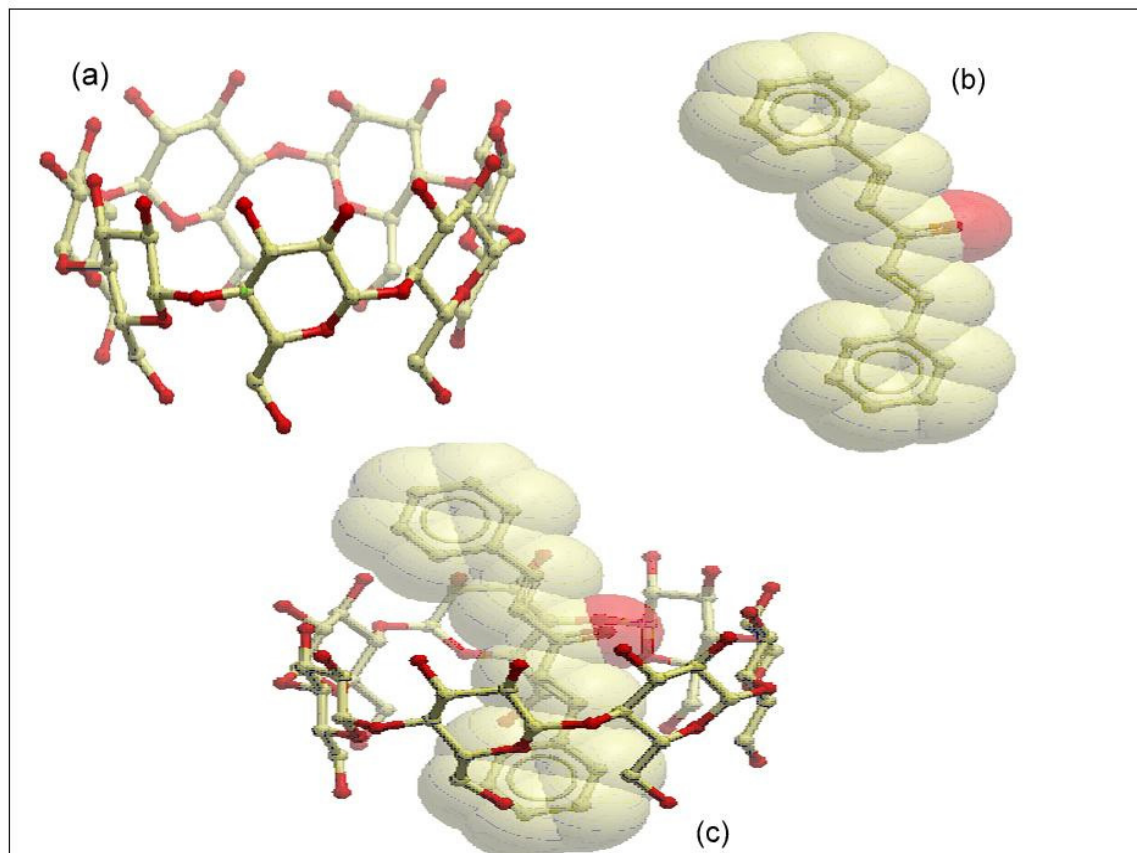
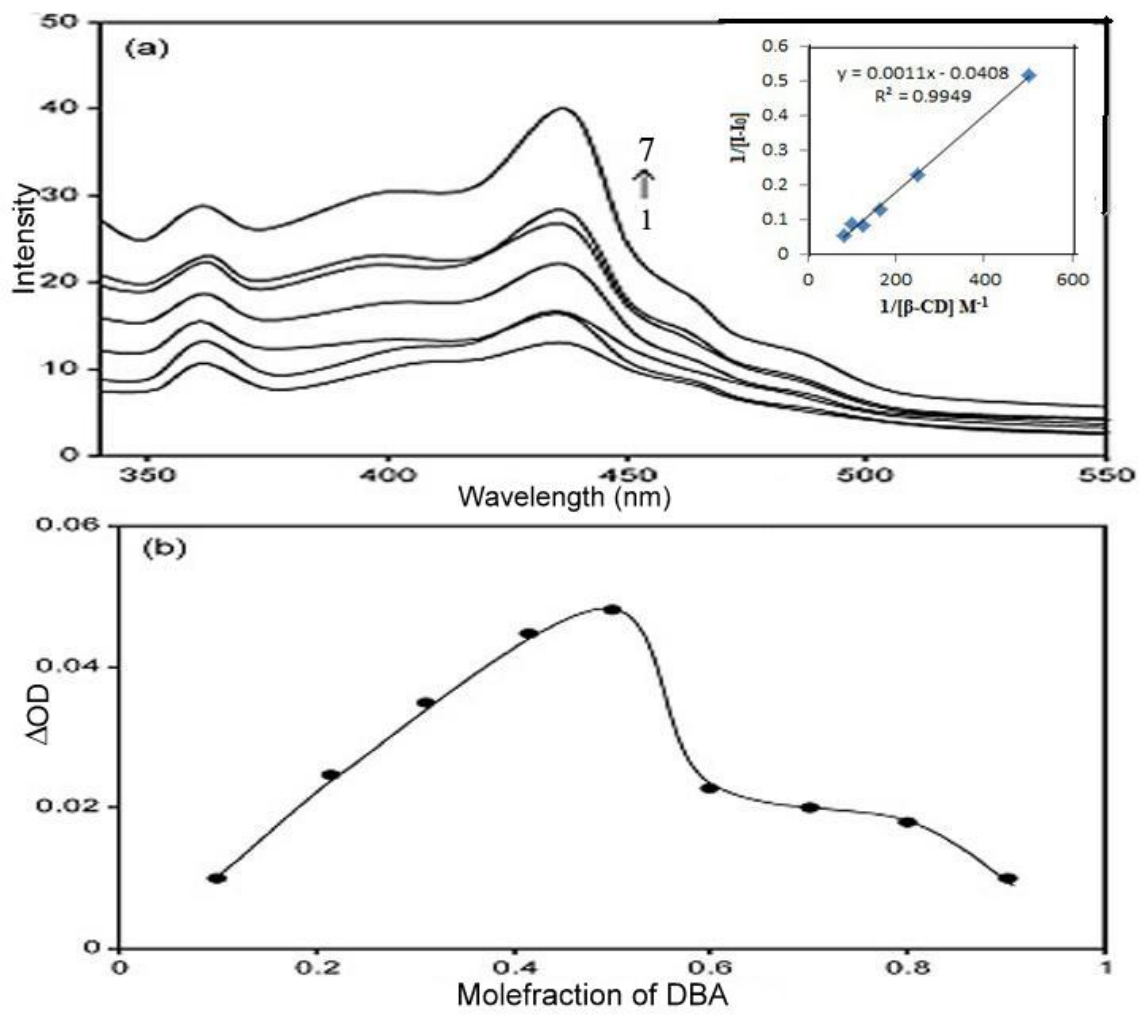
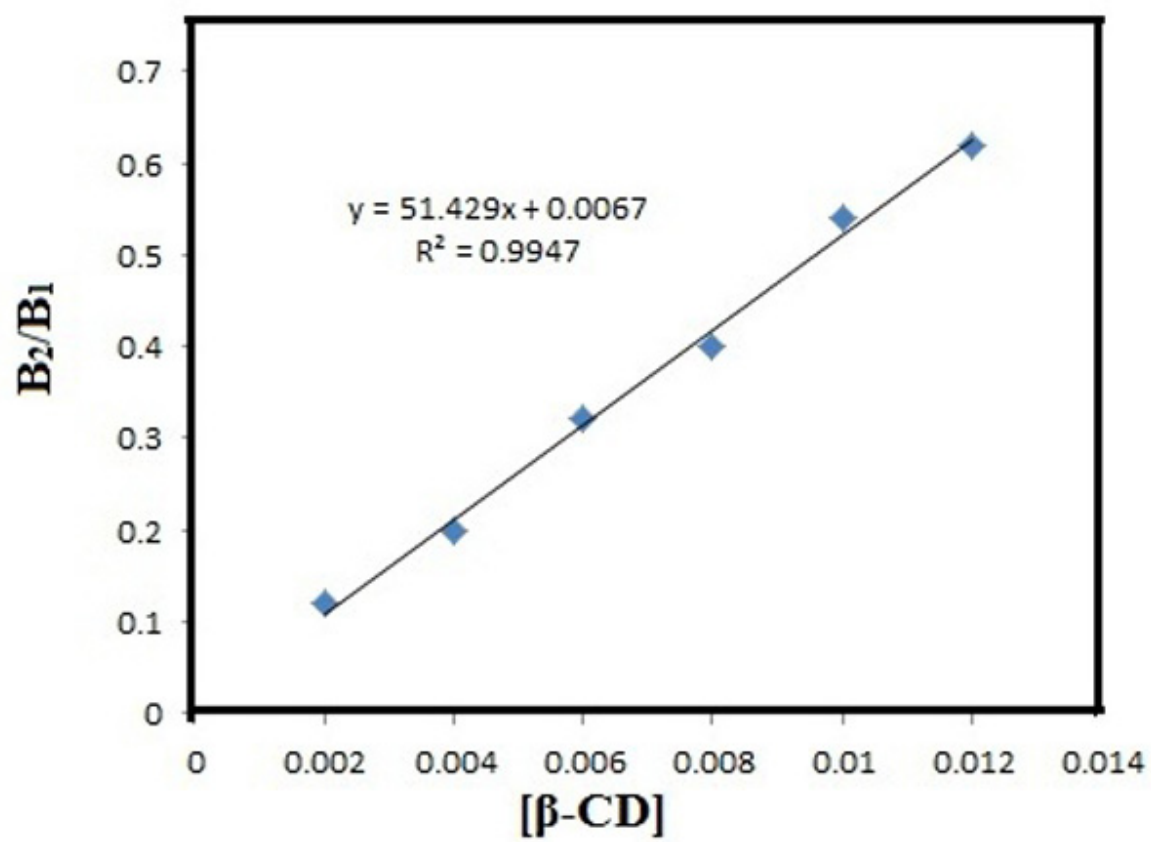


**Fig 8.** Ball and stick representation of (a)  $\beta$ -CD (b) DBA (c) 1:1 inclusion complex; the oxygen atoms are shown as red, carbon atoms are shown as golden balls and sticks, and hydrogen atoms are not shown.

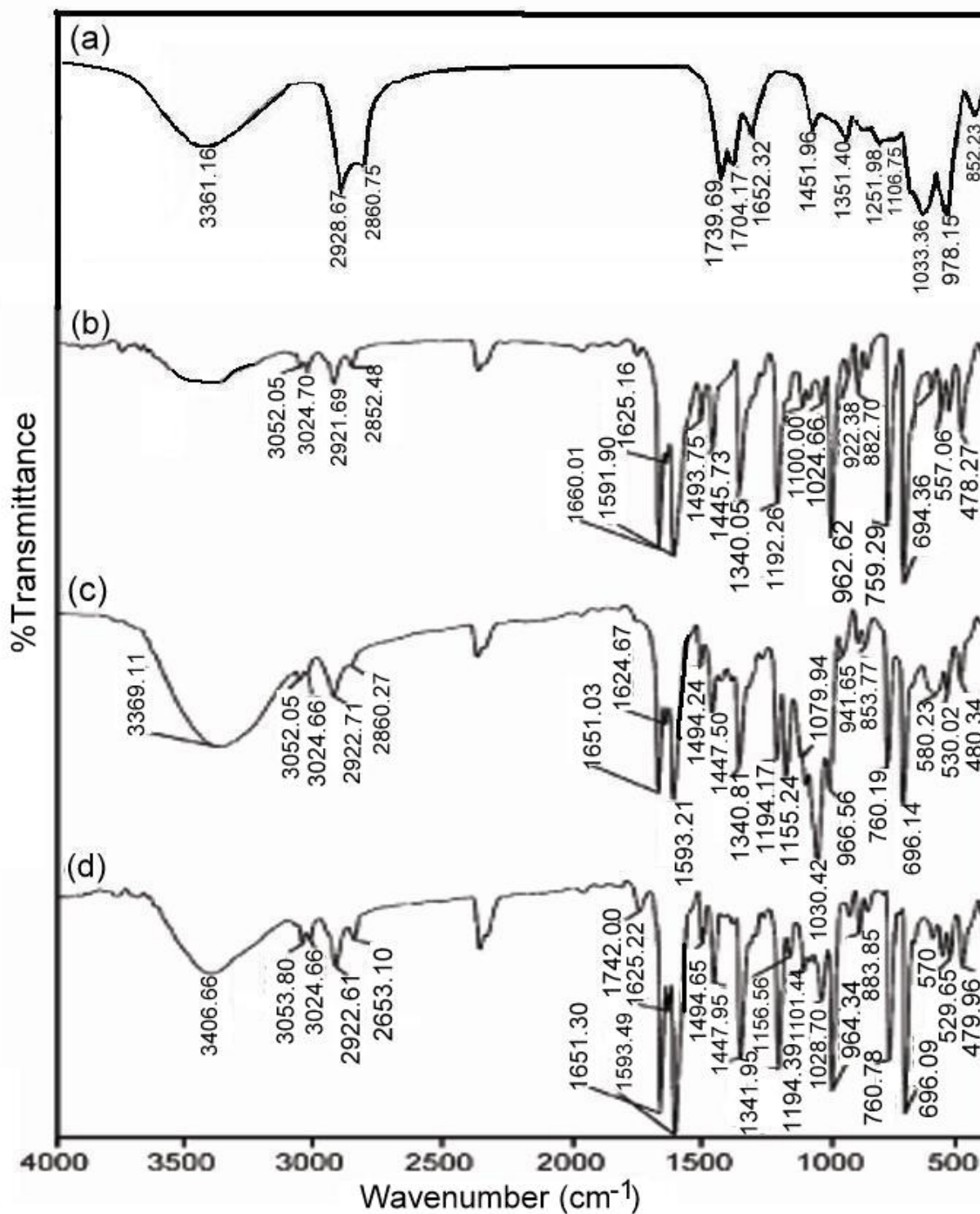


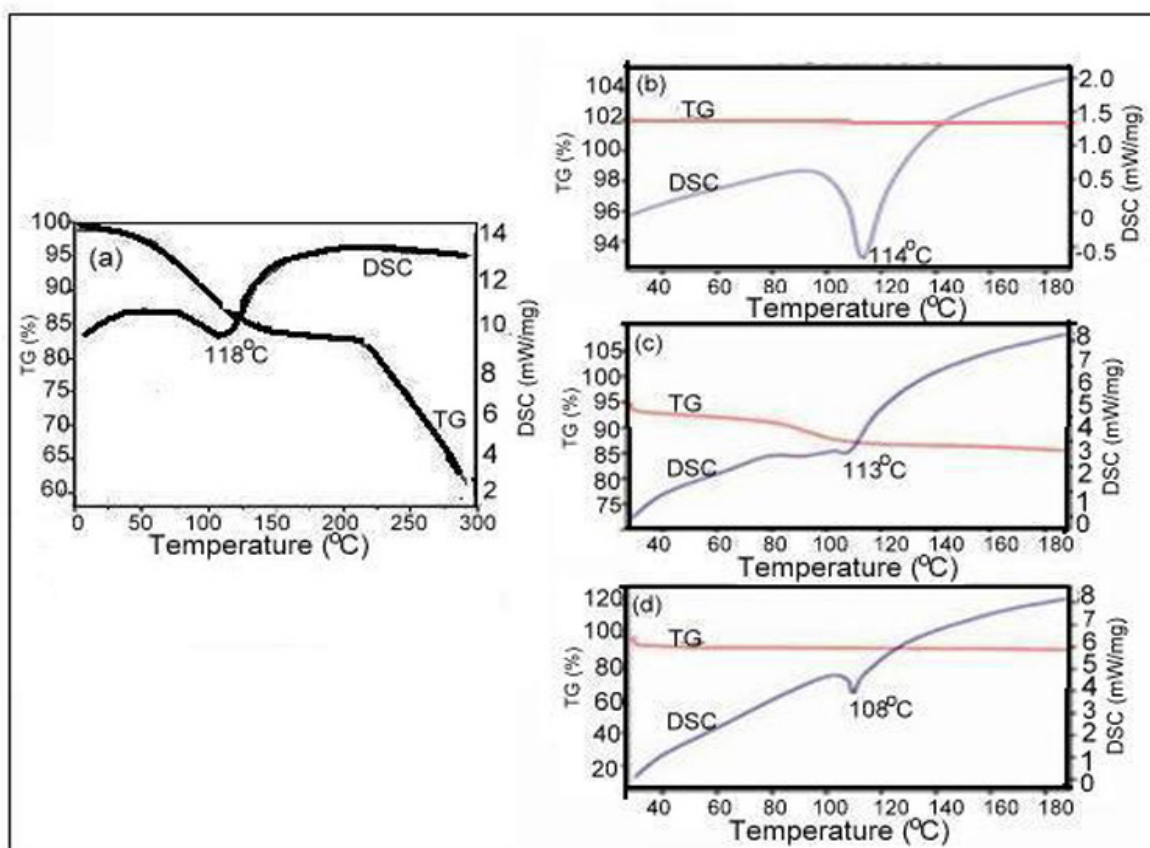


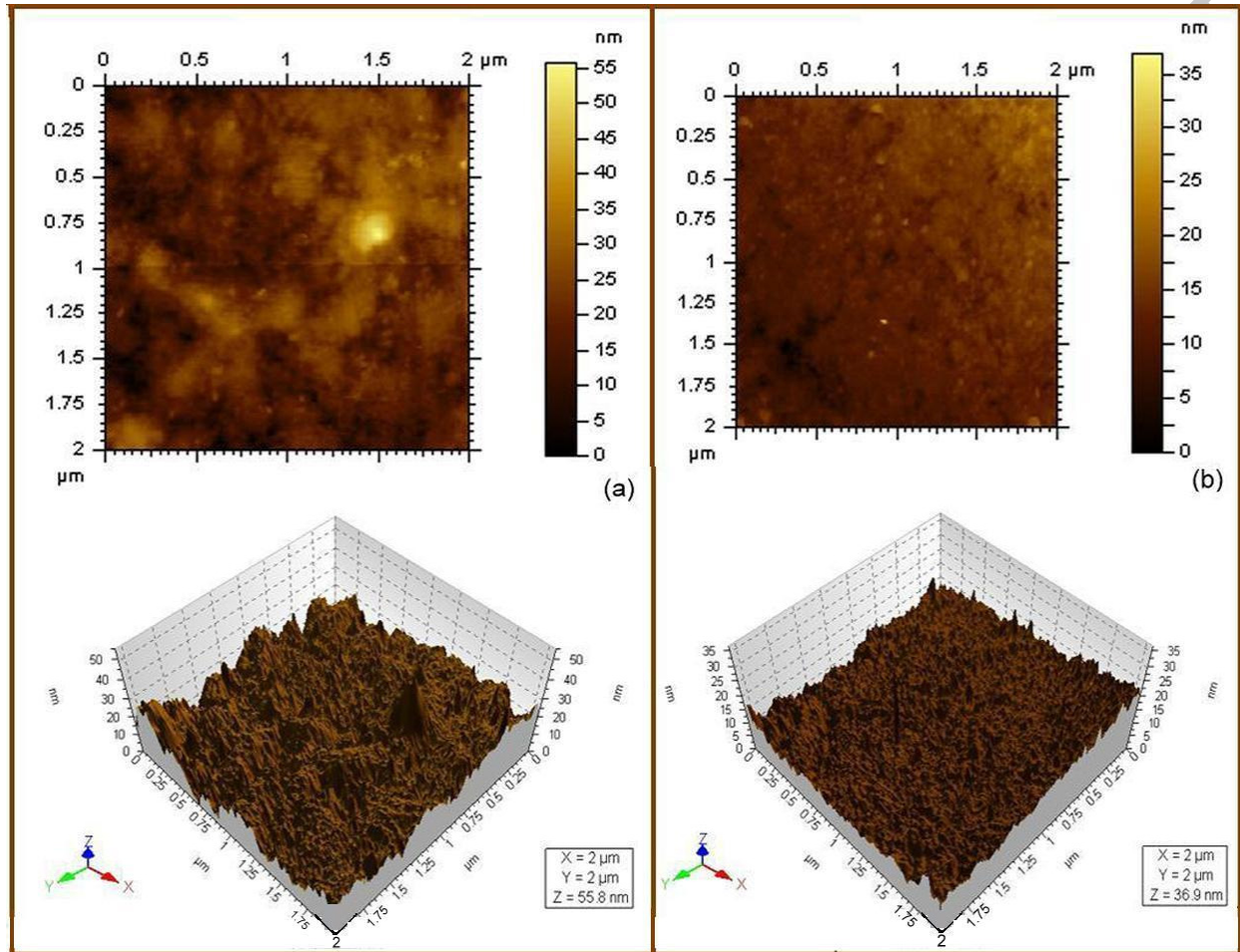
ACCEPTED



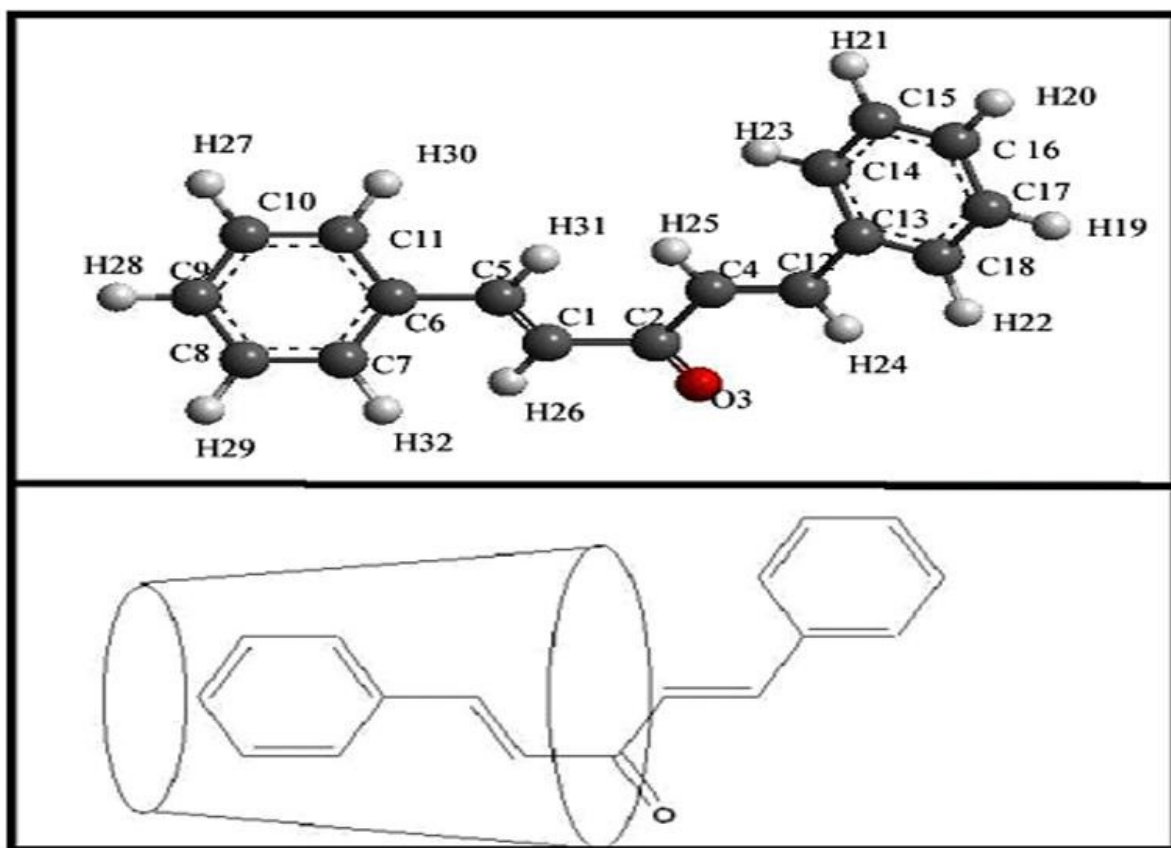
ACCEPT







Graphical abstract



### Highlights

1. Benesi-Hildebrand and Job's plots show the stoichiometry of DBA: $\beta$ -CDx complex 1:1.
2. FT-IR and XRD study confirm the formation of DBA: $\beta$ -CDx inclusion complex.
3. Surface differences in AFM images also provide additional support of complex formation.